

ADVANCED MODELLING TECHNIQUES for AEROSPACE SMEs

Intermediate report

Deliverable 8.1: “Simulation of the LHP in orbital conditions”

1.1 Introduction

The loop heat pipe (LHP) is a closed system in which heat dissipated by two-phase processes, such as evaporation and condensation. It transfers heat from a source to a sink with a small temperature gradient. In the evaporator a porous wick is providing the capillary pumping of the fluid in the loop.

The Loop Heat Pipe features has made it an important, often enabling, two-phase heat transport device for emerging spacecraft and terrestrial thermal control applications.

In this report the transient operation of an innovative propylene LHP is analyzed. Because of using propylene instead of a commoner ammonia LHP, the device is able to reach the lowest temperature preventing the freezing problem in the radiator. The employing of heaters is avoided making the LHP a full passive device. However, when substituting ammonia with Propylene as working fluid it is important to consider some changes like the increase of LHP mass and dimensions.

For the first deliverable of ANTASME, the research group of Thermofluid-dynamics of the University of Bergamo has carried out a numerical simulation of the loop heat pipe response under real satellite conditions.

In order to have a concrete example of utilization of such a code, together with the ANTASME partner, Carlo Gavazi Spazio, it was decided to consider the thermal control of the crycoolers for the Alpha Magnetic Spectrometer (AMS), an experiment to search for dark, missing and antimatter on the space Shuttle and the International Space Station Alpha (Figure 1).

Using a numerical code (SINDA/FLUINT) developed by NASA, a global loop model has been designed. SINDA is a network-style (resistor-capacitor circuit analogy) thermal simulator. The user poses a heat transfer problem by creating an arbitrary network of temperature points (*nodes*) connected by heat flow paths (*conductors*). FLUINT is a network-style fluid flow simulator. It can also be combined with SINDA thermal networks to simulate combined thermal/ hydraulic systems. The user poses a problem by creating an arbitrary network of thermodynamic points (*lumps*) connected by fluid flow passages (*paths*). The user may also define heat transfer routes (*ties*) between SINDA nodes and FLUINT lumps to simulate convection.

By default the code predict flow regimes based on local flow characteristics using as reference the *Design Manual for Microgravity Two-Phase Flow and Heat Transfer* (1989) by C.J. Crowley and M.G. Izenon. These regimes are used for pressure drop calculations. The hardware model consists of four different objects: (a) the Cryo-cooler, which transfer parasitic heat from one source of the thermal protection shields to the LHP evaporator; (b) the Evaporator, where the power allows the fluid evaporation; (c) a Radiator panel, in which the power is get to the environment; (d) the Lines, constituted by a vapour line that came out from the evaporator, a condenser line that crosses the radiator and a liquid line that carries back the condensed liquid to the evaporator.

A more detailed fluid-mechanical simulation is implemented to simulate the performance into the wick. It includes flows of the liquid-vapour interface as needed for detailed transients including oscillations and start-up.

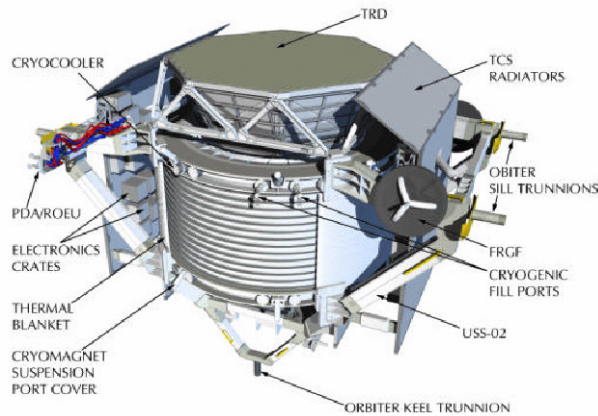


Figure 1 The AMS detector

The heat power and the conductances to the ambient are time varying elements simulating different orbital periods. They have been defined through previous flight conditions which were defined by Carlo Gavazzi Spazio.

1.2 The LHP Model

The LHP configuration studied in this work is schematically presented in Figure 2. Only a quarter of the Zenith radiator is considered, that in the SINDA model is divided in 176 thermal nodes having temperature-varying capacitances. Every LHP is composed by an evaporator, the vapour and liquid line, and a condenser attached to a radiator. The Cryo-cooler transfers dissipated heat from one of the thermal protection shields to 2 evaporators.

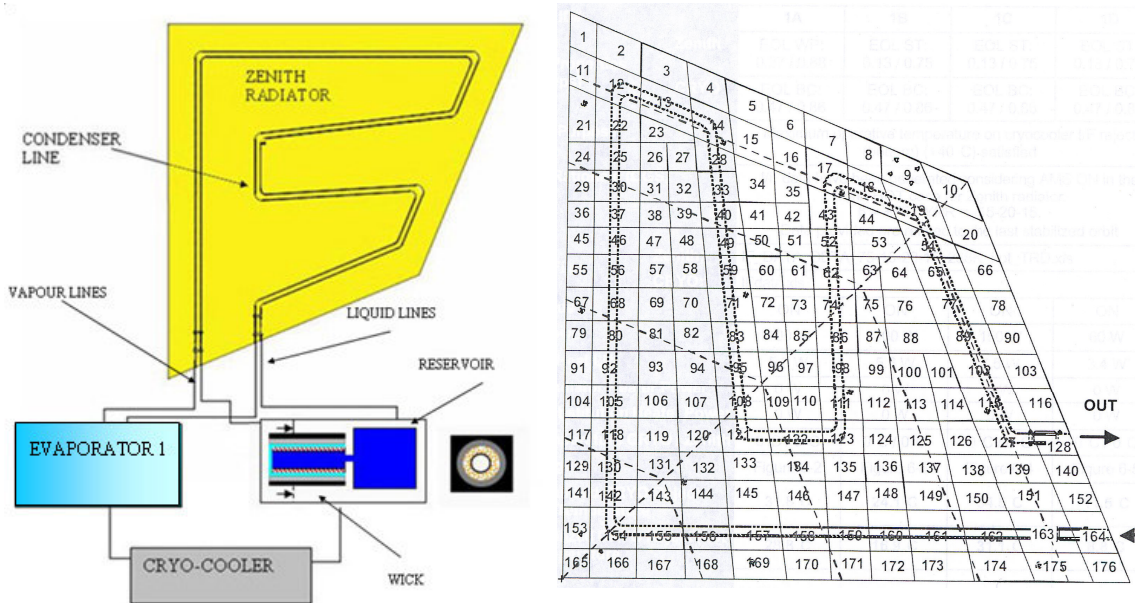


Figure 2. Schematic of the SINDA/FLUINT model on the left, Radiator subdivision in the SINDA model on the right

The global model shown above is broken down into coupled main submodels, corresponding to each type of component: 1) cryo-cooler, 2) evaporator, 3) vapor line, condenser, liquid lines and 4) radiator. In the next paragraphs the implementation of every component in the model is discussed in detail.

AMS includes 4 Stirling Cryogenic Coolers (Cryo-Coolers), which extract parasitic heat from one of the vapour cooled shields. The Cu-collar of the cryocooler is connected via a redundant LHP system to the corresponding quarter of the Zenith radiator. A new cryo-cooler model is implemented in the propylene LHP which account for the last experimental data (Fig. 3).

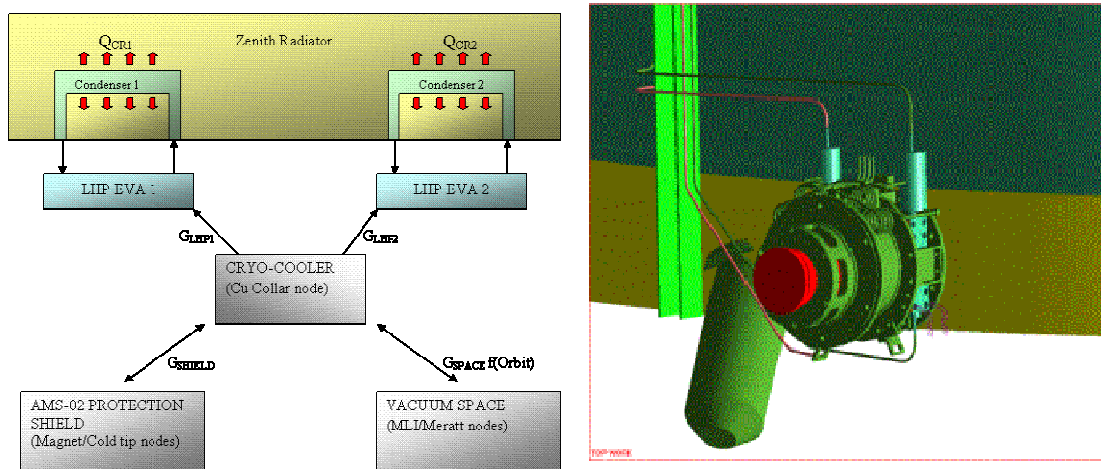


Fig. 3 Nodal diagram of CRYO-COOLER with the conductances on the left; Position of the cryo-cooler in the AMS on the right

The Magnet and the Cold Tip nodes act for interface with the AMS and so they represent only two boundary temperatures for the Cryo-cooler. The MLI and the Merat nodes are the radiative connection with the surrounding space, hence both their temperatures and the radiative conductances are cyclic time depending on the orbital position.

The CRYO COOLER can work in two different ways depending on the working of both the LHP (nominal way) or only one LHP (failure way). In the 2-LHP model, only a half capacitance of the CRYO-COOLER was used. Also the conductance (G_{LHP1} , G_{SHILED} , G_{SPACE}) between the CRYO-COOLER and the other components are considered using one half of their total values. The redundant LHP was disconnected ($G_{LHP2}=0$) and was then considered by doubling the power (Q_{CRI}) from LHP-Condenser to radiator nodes.

In the 1-LHP model, the entire values of the CRYO-COOLER capacitances and conductances are used. The other LHP was thought as a failed LHP, in which only the capacitance of evaporator (included the reservoir and conductance between them) were considered.

The Evaporator configuration consists of cylindrical stainless steel evaporator, imbedded into the rectangular saddle (flange), and reservoir (or compensation chamber) (Fig. 4). The entire loop was thermally insulated to minimize parasitic losses. The pump was embedded into an aluminium saddle so that heat could spread evenly on the upper side of evaporator. Heat input for the evaporator was provided by stainless steel film heaters (equipment), which were attached to the topside of the evaporator saddle.

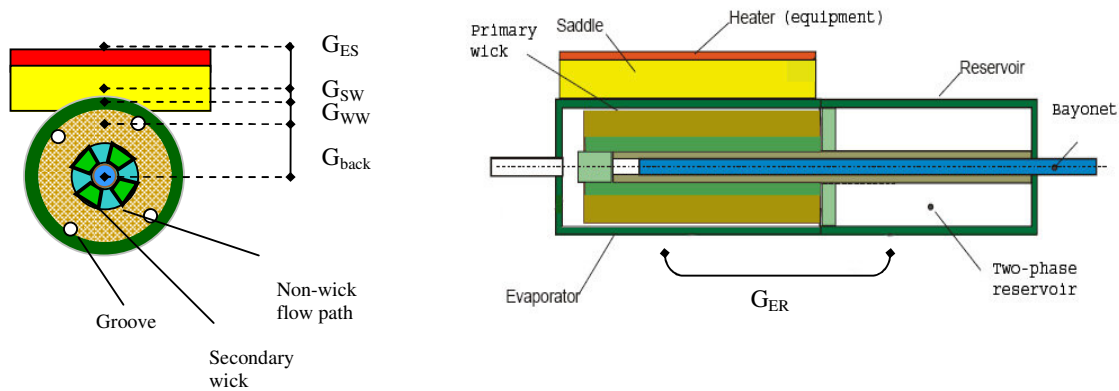


Fig. 4 Evaporator resistances

SINDA/FLUINT uses ad-hoc tools to simulate the evaporator/reservoir physical processes. The fluid is usually shared into 3 nodes (Figure 5): one that accounts for the two-phase reservoir, one for the liquid in the wick and one for the vapour in the grooves. A further grooves node is added to simulate the grooves path.

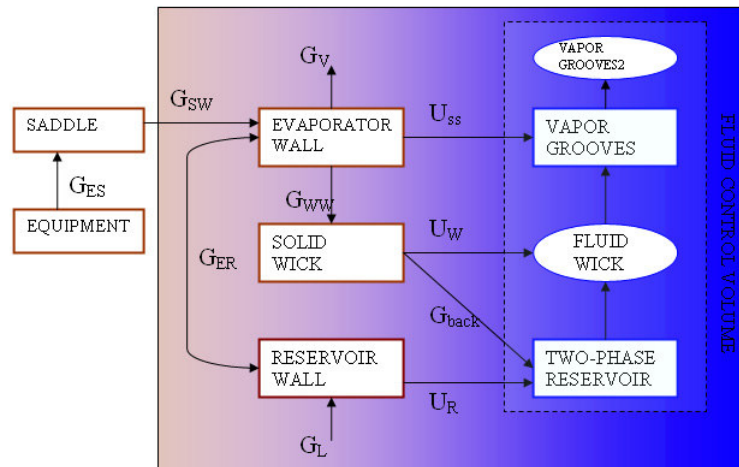
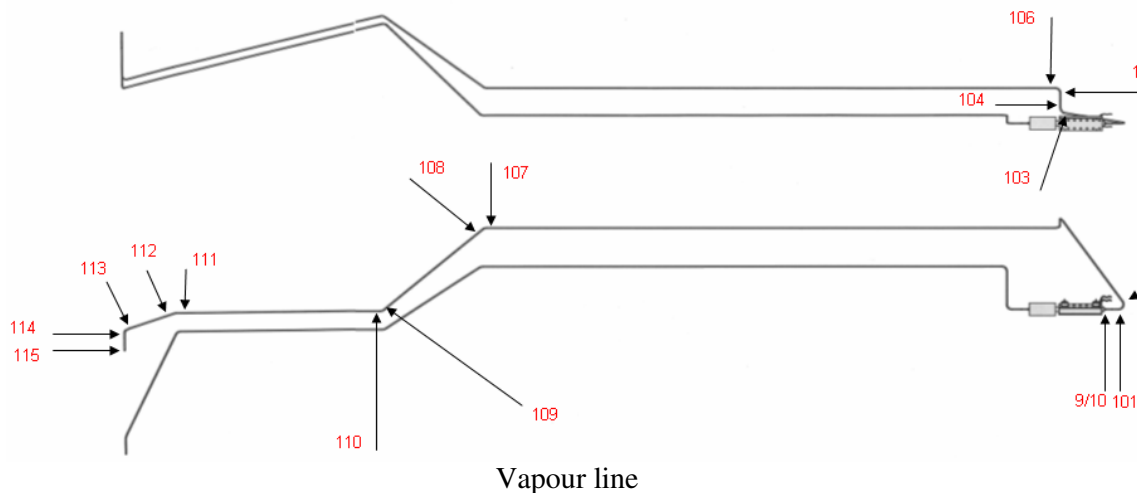
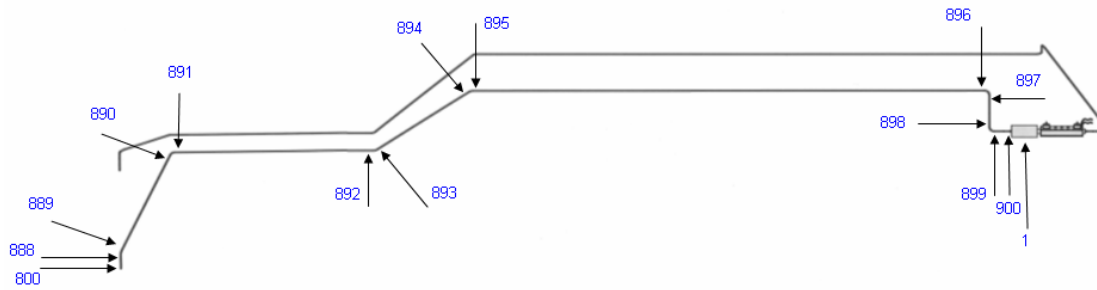


Fig. 5 Conductances inside the evaporator

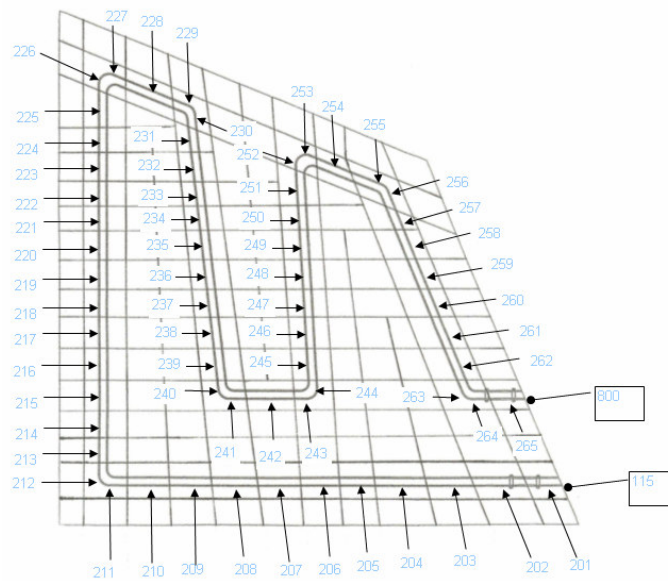
The corresponding solid part is set by inserting three nodes: the evaporator wall, the solid wick (both the primary and secondary wick) and the reservoir wall. The introduction of every node is justified by simulating a heat transfer path inside the evaporator: the evaporator wall accounts for the superheat of the vapour by the U_{ss} heat transfer coefficient, the solid wick is linked to the fluid wick and the reservoir to represent the evaporation (U_W coefficient) and the heat leak (G_{back} conductance) respectively, and the reservoir wall accounts for the solid thermal contact with the evaporator wall and the heat transfer towards the two-phase reservoir.

The working fluid is transported between the various constituents of the system by three liquid lines as shown in figure 6: vapour (stainless steel), condenser (aluminium) and liquid lines (stainless steel).





Liquid line



Condenser line

Fig. 6 Line nodes positions

In microgravity three generalized regimes are recognized: bubbly, slug and annular. The distinction between regimes is based (1) on the liquid and vapour mass fluxes, (2) on the void fraction, (3) on the hydraulic diameter of the line (4) on the magnitude of a body force (or acceleration) vector and its orientation with respect to the duct, (5) on fluid properties such as densities, viscosities, and surface tension, and (6) in the event no clear determination can be made, on previous flow regimes (i.e., regime boundaries exhibit hysteresis).

Single-phase pressure drops are calculated using a Darcy friction factor. A function from Churchill is used to analytically represent the Moody chart. Curved passages result in secondary flows that increase pressure drop. The radius of curvature (the default is 1.0E30 meaning a straight duct) is supplied so that laminar and turbulent friction factors are applied, as well as correlations for critical Reynolds number.

The heat transfer coefficient for laminar flow is obtained by setting the isothermal circular Nusselt number ($Nu=3.66$). For turbulent flow the common Dittus-Boelter correlation is used. Hausen's transition correlation is used for Reynolds numbers between approximately 2000 and 6400.

In two-phase flows, in bubbly and slug flow regimes the predicted pressure drops are based on the McAdam's formulation for homogeneous flow. When the regime is determined to be annular, the Lockhart-Martinelli correlation is used. Both McAdam (homogeneous model), and Lockhart-Martinelli (as Friedel model too) give good predictions for pressure drop in microgravity. Two fundamental boiling heat transfer regimes are recognized: nucleate and

film. The assumption of pure nucleate boiling cannot be made above the critical heat flux or above the corresponding critical wall temperature (Leidenfrost). The critical heat flux and Leidenfrost heat flux are calculated using Zuber's estimates. The basis of the nucleate boiling correlation is Rohsenow's correlation for pool boiling. The high quality film boiling correlation is simply the single-phase Dittus-Boelter correlation for vapour using the current vapour mass fraction and void fraction. The correlation available in the heat transfer calculations in condensation is based on Shah's correlation (that was successful tested with a rectangular duct in microgravity. The heat transfer coefficients in microgravity are 50% less than the correspondent in normal gravity when the flow pattern is bubbly, slug or transitional. In that case a parameter that cut 50% heat transfer coefficient's value can be imposed. All the correlation used smooth transitions into the single-phase regimes to avoid numerical instabilities.

1.3 Boundary conditions

The primary external factor in the thermal environment is solar illumination. This depends primarily on the angle between the ISS orbital plane and the direction to the Sun. The "beta" angle is illustrated in Fig. 1a. For the ISS orbital inclination (51.6°) and the tilt of the Earth's axis (23.5°), the beta angle varies between -75.1° and $+75.1^\circ$, modulated by the seasons as shown in Fig. 1b.

For beta angles with magnitudes greater than 70° the orbit is entirely in sunlight, while for beta angles near 0° about 40% of the orbit is in the Earth's shadow (Fig. 7b). For the majority of the time, the beta angle lies within -50° to $+50^\circ$. The intensity of the solar illumination, or solar constant, also varies annually with the distance to the sun, from 1322 to 1424 W/m^2 at closest approach.

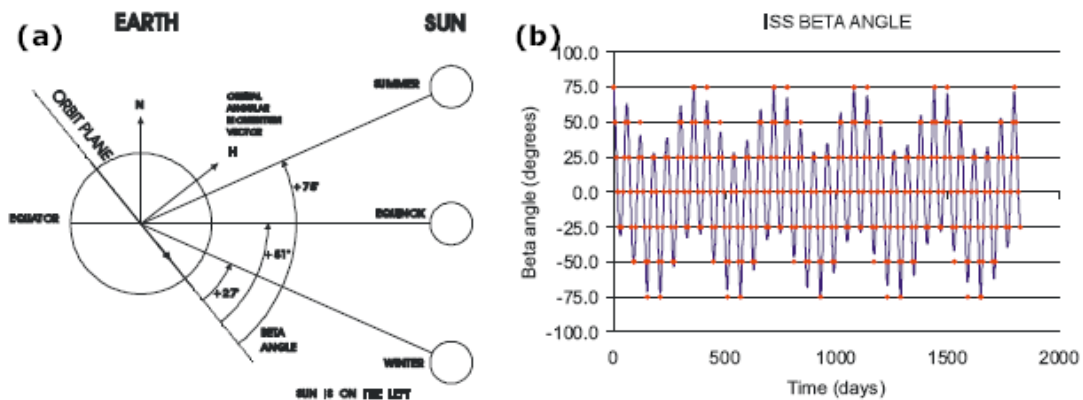


Fig. 7 Beta angle definition (a) and variation (b).

Different parts of AMS are exposed to different amount of direct sunlight at different times, depending on the ISS attitude, which is expressed in the aeronautical coordinates of yaw, pitch and roll.

These are expected to vary by up to $\pm 20^\circ$. Complicating this is the shadowing, in some attitudes, of parts of the experiment by different parts of the space station and the radiation reflected onto different parts of the experiment by different space station elements. The ISS altitude can also vary from 277 to 500 km.

Heat from the Earth is accounted for in two ways. The temperature of the Earth as seen from space varies from 245 to 266 K. The albedo constant, which is associated with reflected solar radiation also varies from 20 to 40%.

In addition, the thermo-optical properties (emissivity and absorptivity) of the exposed experimental surfaces change with time. Internally to the experiment, the thermal environment is also complex. Different parts account for the overall AMS power dissipation requirements.

The time-varying boundary conditions (sink temperatures and external heat fluxes) and thermal coupling between the LHP system and the orbit environment for both cryocooler and radiator are defined by AMS-02 thermal group (Carlo Gavazzi Space) and used to simulate the operation of LHP system on orbit of AMS-02, including the shading effects of the ISS moving parts. Considering the influence of external loads as well as the ISS and internal loads on AMS-02(cryocoolers), the orbit environment, varying with Beta angle and ISS attitude, a system level model is established. Finally, for the LHP system, 21 cases are selected as a subset of the full factorial scan of 7 possible beta angles (from -75° to $+75^\circ$ with the interval equal to 25°) and each one of the three Euler Angles (Yaw, Pitch and Roll) considered at their maximum value, their minimum and an average one, corresponding to the Minimum Propulsion Attitude (MPA).

For each Beta angle we have selected the hottest and the coldest attitude, as well as the MPA one, thus coming to the 21 cases mentioned before.

The hottest case occurring on attitude of Beta angle $=+75^\circ$, Y/P/R $=-15/-20/-15$ and the coldest case on attitude of Beta angle $=+75^\circ$, Y/P/R $=-15/+15/+15$: they are both orbits without eclipse, for which a suitable roll angle provides either a constant pointing to the sun of the zenith radiator (extreme hot case) or a continuous pointing to the deep space (coldest case).

1.4 Cryo-cooler

The magnetic field for the AMS-02 tracker subsystem is provided by a system of superconducting coils placed around the tracker itself. The coils use a classical superconducting alloy of nickel and titanium, so the magnet has to be cooled down to just a few Kelvin to become superconducting.

Since this is a lot colder than the ambient environment of the Space Station, the magnet has to be cooled actively. The principal coolant is a volume of superfluid helium in a tank kept in indirect thermal contact with the magnet. Heat from the magnet is conducted into the superfluid helium where it is consumed by boiling superfluid helium. Ultimately, heat is removed from there by venting this induced helium vapor into space. But since the amount of helium is limited, this can become the limiting factor that finally determines the end of the experiment at large. To avoid that as long as possible AMS-02 is equipped with 4 cryo coolers — heat pumps based on the principle of the Stirling cycle of classical thermodynamics, and designed to operate at the temperatures of the outermost thermal shield layer of gaseous helium.

These heat pumps are operated under some rules and conditions. One of these requires is related to temperature as showed in the following table:

Min. turn-on and operational temperature of the Cryo-cooler	-10°C
Max. operational temperature of the Cryo-cooler	$+40^\circ\text{C}$
Min. non-operational and survival temperature of the Cryo-cooler	-40°C
Max. non-operational and survival temperature	$+40^\circ\text{C}$

Table 1 Cryo-cooler requirements

Due to the necessity to cool the helium and to the electronic in the tracker and in the cryo itself a heat rate come from the cryo-coolers to the LHP. The allocated power budget is a

number representing the mean power to be delivered to cryo-cooler during operation. The common dissipations are showed in the next table.

Minimum	63 W / cryo-cooler
Maximum	158 W / cryo-cooler
Nominal	105 W / cryo-cooler

1.5 Results

The next graphic shows the cryo-cooler temperatures for the 21 different boundary conditions with the nominal power input (105 W). For every beta angle it has been selected the hottest and the coldest attitude, as well as the MPA one.

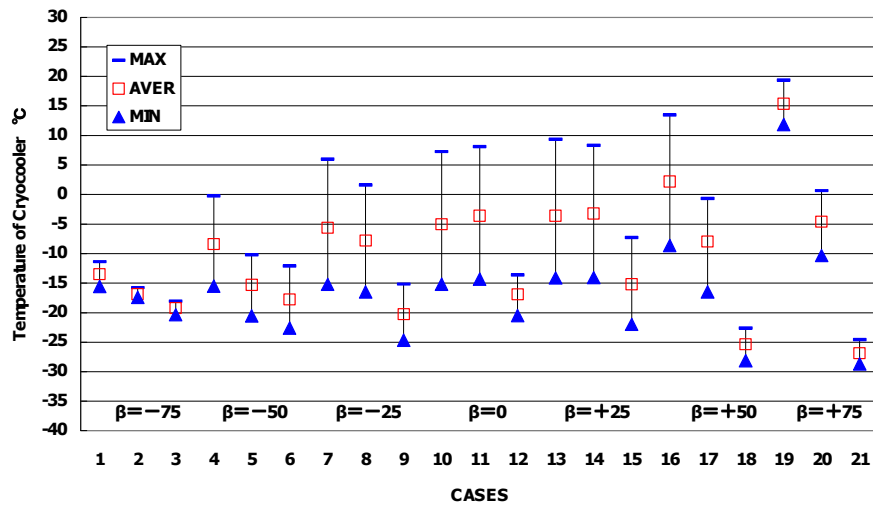


Fig. 8 Thermal analysis of the 21 cases on ISS

The results evidence that all the coldest cases have temperatures lower than the minimum operational temperature in the cryo-cooler (-10°C). The upper limit (+40°C) is not exceeded even in the hottest environment. The worst boundary conditions are achieved with beta angle equal to +75. The related temperatures in the cryo-cooler as well as in the 176 radiator nodes are depicted in the next figures.

- Nominal Operation Analysis

An on-orbit simulation of LHP system for nominal dissipation under the hottest case (Beta angle = +75°, Y/P/R = -15/-20/-15) is shown in Fig. 9, from which we can find the temperature of cryocooler is fluctuating from 11.9°C to 19.3°C due to the variation of orbit environment but still within the required range, and temperatures of radiator are in the range of [-20.8°C, +4.2°C].

The analysis for the coldest case (Beta angle = +75°, Y/P/R = -15/+15/+15) are shown in Fig. 10. Under this environment, the cryocooler temperature would be below its minimum operational temperature -10°C and reaching almost -30°C for some orbit time.

The simulation of worst hot case (hottest environment and maximum dissipation 158W) and worst cold case (coldest environment and minimum dissipation 63W) are presented in Fig. 11 and Fig. 12.

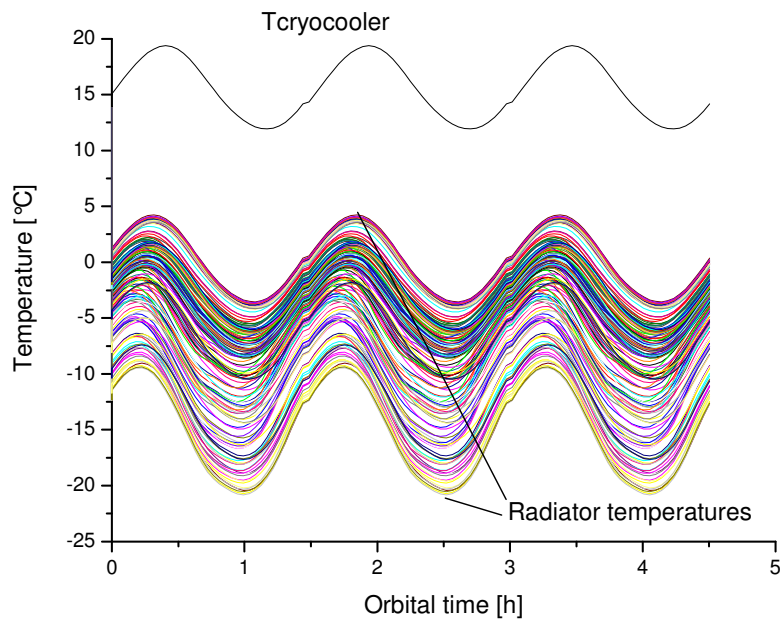


Fig. 9 Nominal analysis results under the hottest environment

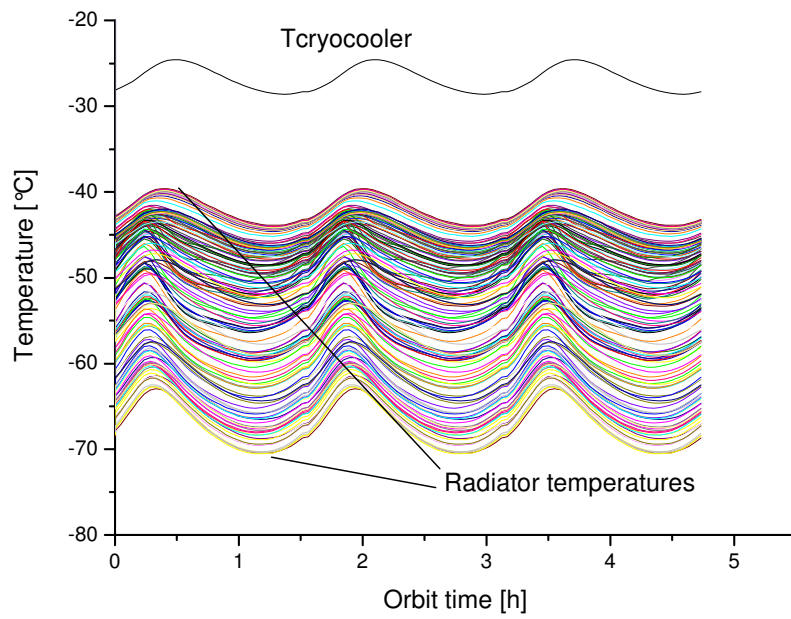


Fig. 10 Nominal analysis results under the coldest environment

1.6 Worst Cases Analysis

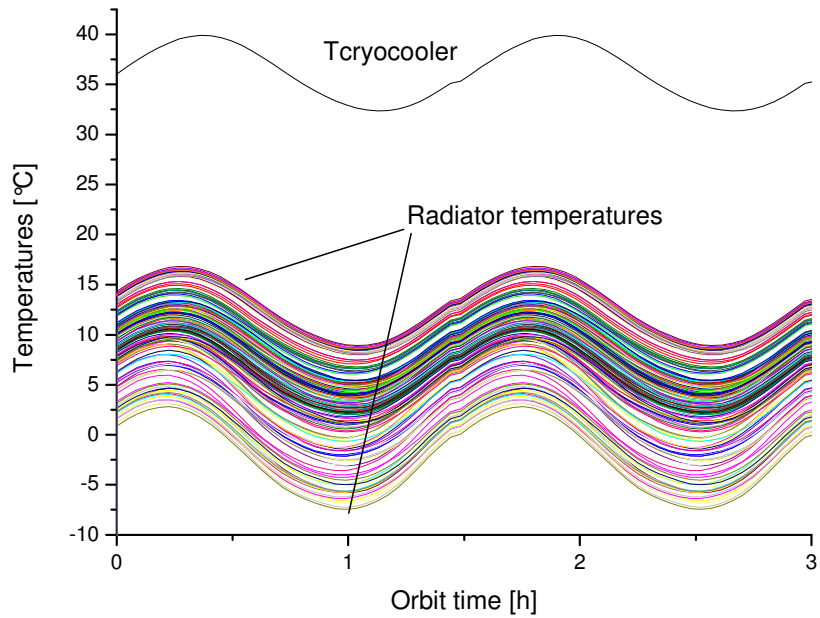


Fig. 11 Hottest Case Analyses with Maximum Power

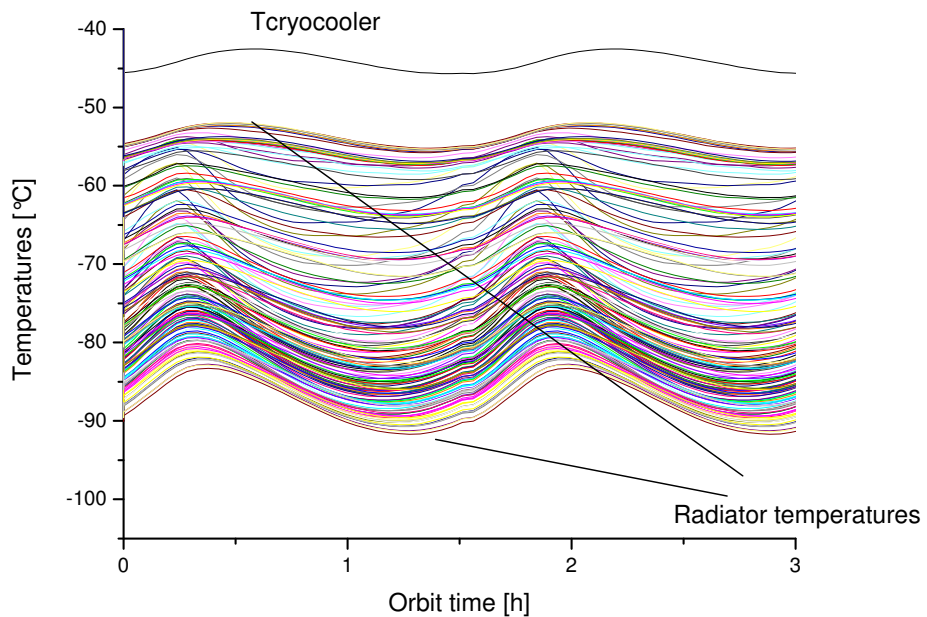


Fig. 12 Coldest Case Analyses with Minimum Power

The proposed propylene LHP system can transfer 158W from cryocooler under the hottest environment, and get the maximum temperature of cryocooler of +39.9°C; however, for the

coldest environment with minimum dissipation of 63W, the cryocooler temperature is much lower than -10°C , reaching -45.7°C . Freezing problem will not occur in the condenser of LHP even in -90°C , because of the low freezing point of propylene.